Available online at www.sciencedirect.com
ScienceDirect
Journal of Sound and Vibration 306 (2007) 172–191
JOURNAL OF SOUND AND VIBRATION
www.elsevier.com/locate/jsvi

The modal and flow velocity corrections of microphone turbulence screens

J.L. Davy[a,b,*]

[a]RMIT University, School of Applied Sciences, GPO Box 2476V, Melbourne, Vic. 3001, Australia
[b]Commonwealth Scientific and Industrial Research Organisation, Manufacturing and Materials Technology, P.O. Box 56, Highett, Vic. 3190, Australia

Received 3 January 2007; received in revised form 22 March 2007; accepted 13 May 2007
Available online 19 June 2007

Abstract

Microphone turbulence screens are used to suppress turbulent pressure fluctuations when measuring the acoustic pressure inside a duct with flow. They consist of a long tube with a slit covered with porous material, and thus are also called sampling tubes. Because they are not omnidirectional, it is necessary to calculate corrections when higher-order modes are propagating in the duct. In order to calculate these corrections it is necessary to know the directivity of the microphone turbulence screen, the propagation direction and energy of the duct modes and the flow velocity of the air in the duct. This paper derives a theoretical formula for the directivity of a microphone turbulence screen. It shows that this theoretical formula agrees better with experimental directivity data than the previously used empirical directivity formula. Because the empirical directivity formula is not a function of the flow velocity, previous research has separated the modal correction from the flow velocity correction. It is shown that it is not theoretically valid to separate the corrections, and that doing so can lead to large errors at high frequencies in the outlet duct. A new method of calculating the modal correction with flow is presented. This method uses a statistical room acoustics approach in contrast to the deterministic numerical approach of the older method. The new method requires much less computing. It is shown that the new method agrees fairly well with the old method for modal corrections without flow. The new method is compared with experimental measurements of the combined modal and flow velocity corrections. Although the trend is the same, the experimental results are higher than the theoretical results in the mid frequency range. The new method agrees reasonably well with the corrections given in ISO 5136:2003.

1. Introduction

Microphone turbulence screens (see Fig. 1) are used to suppress turbulent pressure fluctuations when measuring the acoustic pressure inside a duct with flow. They consist of a long tube which is typically about 400 mm long and 13 mm in cross-section. Normally, there is a 13 mm diameter microphone at one end and a reflecting surface at the other end, which is often fitted with an external nose cone. The screen has a narrow

*Corresponding author at: RMIT University, School of Applied Sciences, GPO Box 2476V, Melbourne, Vic. 3001, Australia. Tel.: +61 422 171 812; fax: +61 3 9925 5290.
E-mail address: john.davy@rmit.edu.au

0022-460X/$ - see front matter © 2007 Elsevier Ltd. All rights reserved.
doi:10.1016/j.jsv.2007.05.016

Nomenclature

a_y, a_z	internal dimensions of rectangular cross-section duct
a	specific acoustic admittance ratio
a_1, a_2	boundary condition constants
A	microphone turbulence screen internal cross-sectional area
b	microphone turbulence screen slit width
c	speed of sound in air
C	modal and velocity correction factor
d	distance from duct wall
d_y, d_z	distance of measurement rectangle from walls of duct
D	diameter of cylindrical duct
e	exp(1)
E	complex amplitude of external sound pressure wave
f	frequency
$f(\theta)$	desired ideal pressure squared response
F	effective length ratio of microphone turbulence screen
g	$\sqrt{1+(2\beta_0/k_0)^2}$
G	$-2\mathrm{i}k_0\beta_0$
H	increase in average pressure squared value due to reflection at wall
i	square root of minus one
i	unit vector in direction of positive x-axis
int()	function that produces the integer part of a number
j	integer
$J_1()$	Bessel function of the first kind of order one
k	wavenumber amplitude
k_0	ω_0/c
k_1	real part of wavenumber inside screen
k_c	wavenumber at third octave band centre frequency
k_j	values of wavenumber used to calculate average
k_p	magnitude of wavenumber projection onto duct cross-section
k_x, k_y, k_z	components of wavenumber in x, y and z directions
k	wavenumber vector
$\mathbf{k}_{mn}$	projection of wavenumber of duct mode onto duct cross-section
K	empirical directivity constant
K'	empirical directivity constant
L	length of microphone turbulence screen slit
m	complex wavenumber inside screen or duct mode index
m_1	complex wavenumber inside extension tubes
M	Mach number
n	duct mode index
N	number of points used to calculate third octave band average
$N(k_p)$	number of duct modes with wavenumber projection less than k_p
p	complex sound pressure amplitude
p_i, p_r	incident and reflected sound pressure waves
p_x	complex external sound pressure amplitude at slit
p_0	complex amplitude of external sound wave
$p(t, \mathbf{x})$	external sound pressure at time and position **x**
P	sound pressure
q	complex amplitude of rate of volume addition per unit volume
$q, q+\Delta q$	limits of small range of k_y values
Q	rate of volume addition per unit volume
r	specific airflow resistance
R	relative measurement radius
S	cross-sectional area of duct
t	time
v	velocity of external moving media
v	velocity vector of external moving media
$w(\theta)$	angular distribution of sound energy in duct
x	spatial position vector relative to external moving media
x_0	spatial position on x-axis relative to stationary coordinates
$\mathbf{x}_0$	spatial position vector relative to stationary coordinates
x, y, z	spatial variables
Z_s	specific acoustic impedance of surface
β_0	$\rho_0 cb/(2rA)$
β_{01}	value of β_0 in extension tubes
β_1	attenuation of sound pressure per unit distance inside screen
θ	angle of incidence of sound
ρ_0	ambient density of air

ω	angular frequency when moving with external media	∇^2	Laplacian operator
		$\partial/\partial n$	normal gradient into surface
ω_0	angular frequency at stationary point	$\langle\,\rangle$	average value

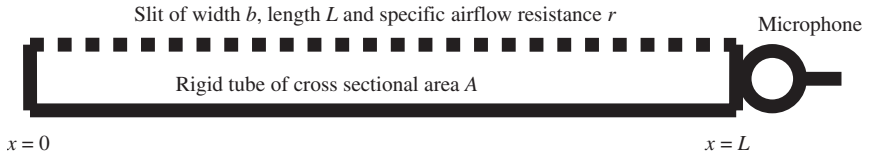

Fig. 1. Microphone turbulence screen.

(~1 mm) slit, which runs the full length of the tube and is covered with porous material, or is manufactured from a porous material. They are also called sampling tubes.

The research work described in this paper arose out of a research project to develop a flush mounted microphone turbulence screen for use in a power station chimney flue. The development project required the determination of the sound pressure at the inside wall of the chimney flue. Thus, the modal and flow velocity corrections in the International Standard ISO 5136 [1,2] could not be used. The corrections in ISO 5136 are for estimating the sound power propagating along a duct and thus assume a desired microphone sound pressure squared response proportional to the cosine of the angle of incidence relative to the axis of the duct. For the development project, the desired microphone response was omnidirectional. Hence, the modal corrections would have larger magnitude. Thus new modal and velocity corrections had to be calculated. A new method of calculating these corrections was developed and it was shown that the modal and velocity corrections could not be separated as is done in ISO 5136:1990 [1]. The new method is presented in full in this paper. Since the development of the method described in this paper, ISO 5136:2003 [2] has been published. The new version of the standard contains combined modal and flow velocity corrections, which were calculated using a significant improvement of the method used to calculate the modal corrections in the earlier version. The improved method is different from the method described in this paper.

The microphone turbulence screen which was developed used anechoic terminations in conjunction with a flush mounted microphone. This is in contrast to the conventional microphone turbulence screen, which uses reflecting ends, one of which is the microphone diaphragm. The new method of calculating the modal and velocity correction was applied to a conventional microphone turbulence screen and used to calculate the corrections for estimating the sound power flowing down a duct. In order to do this, a Waterhouse style correction taking account of the variation of sound pressure squared across the duct had to be developed. These new corrections were compared to existing theoretical and experimental estimates of the corrections. It was shown that the differences between the theoretical corrections were mainly due to different assumptions about the directivity of the microphone turbulence screen, and the angular distribution of the sound energy in a duct. The theoretical derivation of the microphone turbulence screen directivity was made more exact, and the theoretical directivity formula was shown to agree better with experimental measurements than the previous empirical formulae.

2. Theoretical directivity

The theoretical response of a microphone turbulence screen has been analysed by Neise [3], Wang and Crocker [4] and Michalke [5,6]. The analysis is extended in this paper to cover the case of a microphone turbulence screen with long tubes of the same cross-sectional area at each end of the slit (see Refs. [7,8]). A microphone turbulence screen is shown in Fig. 1. The directional response of a microphone turbulence screen can be determined theoretically by studying the propagation of sound within the microphone

turbulence screen for different external excitations. The wave equation for sound pressure is

$$\nabla^2 P - \frac{1}{c}\frac{\partial^2 p}{\partial t^2} = -\rho_0 \frac{\partial Q}{\partial t}, \tag{1}$$

where P is the sound pressure, c the speed of sound, t the time, ρ_0 the ambient density, and Q the net rate of volume addition per unit volume. If the variation of Q with time is sinusoidal, then P will also be sinusoidal in the steady state. Thus,

$$Q = q\mathrm{e}^{\mathrm{i}\omega_0 t} \quad \text{and} \quad P = p\mathrm{e}^{\mathrm{i}\omega_0 t}, \tag{2}$$

where ω_0 is the angular frequency. The wave equation becomes

$$\nabla^2 p + k_0^2 p = -\mathrm{i}\omega_0 \rho_0 q, \tag{3}$$

where $k_0 = \omega_0/c$ is the wavenumber.

For a microphone turbulence screen with an internal cross-sectional area A of its tube, a slit width b and a porous fabric covering the slit of specific airflow resistance r, the rate of volume addition per unit volume is

$$q = \frac{b(p_x - p)}{rA}, \tag{4}$$

where p_x is the complex external sound pressure amplitude. The specific airflow resistance of the fabric is the ratio of the pressure difference across the fabric to the linear velocity of airflow just outside the surface of the fabric. The one-dimensional wave equation for a microphone turbulence screen is

$$\frac{\partial^2 p}{\partial x^2} + k_0^2 p = -2k_0\beta_0(p_x - p), \tag{5}$$

where

$$\beta_0 = \frac{\rho_0 c b}{2rA} \tag{6}$$

and x is the spatial variable. This equation can be rearranged into

$$\frac{\partial^2 p}{\partial x^2} + m^2 p = G p_x, \tag{7}$$

where

$$m^2 = k_0^2 - 2\mathrm{i}k_0\beta_0 \tag{8}$$

and

$$G = -2\mathrm{i}k_0\beta_0. \tag{9}$$

Taking the square root of Eq. (8) with positive real part gives

$$m = k_1 - \mathrm{i}\beta_1. \tag{10}$$

Define

$$g = \sqrt{1 + \left(\frac{2\beta_0}{k_0}\right)^2}. \tag{11}$$

Then

$$k_1 = k_0\sqrt{\frac{g+1}{2}} \tag{12}$$

and

$$\beta_1 = k_0\sqrt{\frac{g-1}{2}}. \tag{13}$$

If the external sound pressure is sinusoidal in space

$$p_x = E\mathrm{e}^{-\mathrm{i}k_x x} \tag{14}$$

and the wave equation becomes

$$\frac{\partial^2 p}{\partial x^2} + m^2 p = GE\mathrm{e}^{-\mathrm{i}k_x x}. \tag{15}$$

The solution of this equation is

$$p = \frac{GE\mathrm{e}^{-\mathrm{i}k_x x}}{m^2 - k_x^2} + a_1\mathrm{e}^{-\mathrm{i}mx} + a_2\mathrm{e}^{\mathrm{i}mx}. \tag{16}$$

This solution is only valid if β_0 is independent of x. This will always be assumed to be the case in this paper. The first term of the solution is a particular integral of Eq. (15) and the last two terms are the solution of the homogeneous version of Eq. (15). The constants a_1 and a_2 have to be determined from the boundary conditions.

The boundary conditions for a sound wave are

$$\frac{\partial P}{\partial n} + \frac{\rho_0}{Z_s}\frac{\partial P}{\partial t} = 0, \tag{17}$$

where Z_s is the specific acoustic impedance of the surface and $\partial P/\partial n$ denotes the gradient of P in the direction normal to the surface and from the space into the surface. The specific acoustic impedance of a surface is the ratio of the sound pressure at the surface to the particle velocity in the direction normal and into the surface. For a sound pressure which varies sinusoidally with time Eq. (17) can be rewritten as

$$\frac{\partial p}{\partial n} + \mathrm{i}k_0 ap = 0, \tag{18}$$

where the specific acoustic admittance ratio a is given by

$$a = \frac{\rho_0 c}{Z_s}. \tag{19}$$

For a rigid surface a is equal to zero. If the tube continues on to plus or minus infinity, past the ends of the microphone turbulence screen slit that is exposed to the external sound, the sound pressure is given by the second or third term of the right-hand side of Eq. (16) providing an appropriate value β_{01} of β_0 is used. The first term is zero because there is no external sound pressure acting on the tube extension and a_1 or a_2 is zero since there cannot be any sound coming from infinity. At the end of the tube, which extends to plus infinity

$$\frac{\partial p}{\partial n} = \frac{\mathrm{d}p}{\mathrm{d}x} = -\mathrm{i}m_1 a_1 \mathrm{e}^{-\mathrm{i}m_1 x} = \mathrm{i}m_1 p, \tag{20}$$

where m_1 is the value of m in the extension tube. Thus $a_1 = m/k_0$. If the tube extension has no slit then $\beta_{01} = 0$, $m_1 = k_0$ and $a = 1$. If the slit and its covering fabric in the extension tube are the same as the slit and covering fabric exposed to the external sound in the actual turbulence screen, an anechoic termination is obtained. In this case β_{01} equals β_0, and the m_1 for the extension tube is the same as the m for the actual turbulence screen.

If the actual microphone turbulence slit runs from $x = 0$ to L and the specific acoustic admittance ratio is the same at both ends of the slit, the boundary conditions are

$$\frac{\mathrm{d}p}{\mathrm{d}x}(0) = \mathrm{i}k_0 ap(0), \tag{21}$$

$$\frac{\mathrm{d}p}{\mathrm{d}x}(L) = -\mathrm{i}k_0 ap(L). \tag{22}$$

A large amount of tedious algebra enables Eqs. (16), (21) and (22) to be solved for the constants a_1 and a_2, which can then be substituted back into Eq. (16) to obtain the sound pressure at $x = L$. This gives

$$\frac{p(L)}{p_x(L)} = \frac{-2ik_0\beta_0}{m^2 - k_x^2}\left(1 - \frac{2(k_0a + k_x)me^{ik_xL} + (k_0a - k_x)[(m + k_0a)e^{imL} + (m - k_0a)e^{-imL}]}{(m + k_0a)^2e^{imL} - (m - k_0a)^2e^{-imL}}\right). \tag{23}$$

If $a = 0$, Eq. (23) becomes

$$\frac{p(L)}{p_x(L)} = \frac{-2ik_0\beta_0}{m^2 - k_x^2}\left(1 + \frac{k_x}{m}\frac{1 + e^{-2imL} - 2e^{i(k_x - m)L}}{1 - e^{-2imL}}\right). \tag{24}$$

This equation agrees with Eq. (5) of Michalke [5] as modified by the errata. It applies for rigid reflecting surfaces at both ends of the slit. If $a = m/k_0$, Eq. (23) becomes

$$\frac{p(L)}{p_x(L)} = -\frac{2ik_0\beta_0(1 - e^{i(k_x - m)L})}{2m(m - k_x)}. \tag{25}$$

This applies for the case of an anechoic termination at both ends of the slit.

The complex arithmetic can be removed from Eq. (25) by taking the modulus squared of both sides and substituting for m using Eq. (10). The result is

$$\left|\frac{p(L)}{p_x(L)}\right|^2 = \frac{k_0^2\beta_0^2}{k_1^2 + \beta_1^2}\frac{1 + e^{-2\beta_1L} - 2e^{-\beta_1L}\cos[(k_1 - k_x)L]}{(k_1 - k_x)^2 + \beta_1^2}. \tag{26}$$

This equation agrees with Eq. (35) of Neise [3] if Neise's approximations are corrected and his pressure doubling factor is removed. Neise's approximations are $k_1 = k_0$, $\beta_1 = \beta_0$ and $\beta_1 \ll k_1$. The moduli squared of Eqs. (23) and (24) were evaluated by programming computer spreadsheet functions to perform complex arithmetic.

The equation of a plane sound wave is

$$p(t, x) = p_0e^{i(\omega t - \mathbf{k}\cdot\mathbf{x})}, \tag{27}$$

where p is the sound pressure at time t and position $\mathbf{x}$ relative to the medium, p_0 the complex amplitude of the sound wave, ω the angular frequency of the sound wave and $\mathbf{k}$ the wavenumber vector. If the medium is moving at velocity $\mathbf{v}$, then relative to the medium, a stationary point appears to move with a velocity $-\mathbf{v}$. Its position relative to the medium is given by $\mathbf{x}_0 - \mathbf{v}t$, where $\mathbf{x}_0$ is its position relative to stationary coordinates and where the moving medium coordinates correspond with the stationary coordinates at time $t = 0$. The sound pressure at this stationary point is given by

$$p(t, x_0) = p_0e^{i[(\omega + \mathbf{k}\cdot\mathbf{v})t - \mathbf{k}\cdot\mathbf{x}_0]}. \tag{28}$$

If $\mathbf{v}$ is in the direction of the positive x-axis and $\mathbf{x}_0$ is on the x-axis, then $\mathbf{v} = v\mathbf{i}$ and $\mathbf{x}_0 = x_0\mathbf{i}$. The sound pressure is given by

$$p(t, x_0) = p_0e^{i[(\omega + k_xv)t - k_xx_0]}, \tag{29}$$

where k_x is the component of the wavenumber $\mathbf{k}$ in the direction of the x-axis. If the sound wave is travelling at an angle of θ to the x-axis then

$$k_x = k\cos\theta = \frac{\omega\cos\theta}{c}, \tag{30}$$

where k is the amplitude of $\mathbf{k}$ and c the speed of sound. If the Mach number is $M = v/c$, then

$$p(t, x_0) = p_0e^{i[(1 + M\cos\theta)\omega t - kx_0\cos\theta]}. \tag{31}$$

Thus, the angular frequency of the sound wave observed at the stationary point is

$$\omega_0 = (1 + M\cos\theta)\omega. \tag{32}$$

If a stationary microphone turbulence screen is placed along the x-axis in the moving medium and excited by the plane sound wave in the moving medium, the wavenumber k_0 inside the turbulence screen is given by

$$k_0 = \frac{\omega_0}{c} = \frac{(1 + M\cos\theta)\omega}{c} = (1 + M\cos\theta)k \tag{33}$$

and from Eqs. (30) and (33)

$$k_x = \frac{k_0\cos\theta}{1 + M\cos\theta}. \tag{34}$$

The theoretical response and directivity of a microphone turbulence screen can be calculated using Eqs. (23) and (34).

The theoretical response and directivity will not be valid when the cross-sectional dimensions of the turbulence screen become comparable to the wavelength. The response will be inaccurate when the cross-sectional dimensions become equal to a quarter of the wavelength because Eq. (4) fails. This is because the external sound pressure acting through the resistance of the material covering the slit is no longer driving an acoustic volume compliance but the zero acoustic impedance of a quarter wavelength depth. The directivity will be incorrect when the cross-sectional dimensions become equal to half of the wavelength because Eq. (3) will no longer be valid. This is because cross-mode propagation becomes possible and the one-dimensional wave equation is no longer adequate. For the microphone turbulence screens considered in this paper with a typical cross-sectional dimension of 13 mm, this cross-sectional dimension becomes equal to a quarter of the wavelength at 6.6 kHz and half of the wavelength at 13.2 kHz.

3. Modal and velocity correction

A microphone turbulence screen is conventionally calibrated in an anechoic room with zero flow (Mach number M equals zero) and with angle of incidence equal to zero. For non-zero Mach numbers and non-zero angles of incidence a theoretical correction to the calibration must be calculated. If sound is incident from different directions at the same time, the theoretical correction must be averaged over the different angles of incidence with a weighting, which is proportional to the sound energy incident from each direction. This approach assumes that sound incident from different directions is uncorrelated. If the duct is anechoically terminated or has an open end whose dimensions are larger than a wavelength, back reflections can be ignored. This means that it is only necessary to average over angles of incidence from 0° to 90°.

The angular distribution of sound energy in a duct is not normally known. The obvious assumptions that might be made about the angular distribution of sound energy in a duct are that every mode carries equal power down the duct, that every mode has equal energy density, that equal energy is incident from every element of angle of incidence or that equal energy is incident from every element of solid angle. The correction factor $C(\omega,M)$ is calculated by averaging the pressure-squared response $|p(\omega,\theta,M)/p(\omega,0,0)|^2$ of the microphone turbulence screen with the appropriate sound energy angular distribution weighting factor $w(\theta)$ over angles of incidence θ from 0° to 90° and dividing this into the average of the desired angular response with the weighting function. This gives

$$C(\omega,M) = \frac{f(0) + \int_0^{\pi/2} f(\theta)w(\theta)\,\mathrm{d}\theta}{|p(\omega,0,M)/p(\omega,0,0)|^2 + \int_0^{\pi/2} w(\theta)|p(\omega,\theta,M)/p(\omega,0,0)^2\,\mathrm{d}\theta}. \tag{35}$$

The first terms in the numerator and denominator take account of the plane wave mode. For frequencies below the cut on frequency of the first duct cross-mode, the second terms in the numerator and denominator are set equal to zero, because there are no propagating cross-modes. Using Eqs. (35), (23) and (34), $C(\omega, M)$, can be calculated theoretically.

The function $f(\theta)$ is the desired ideal pressure squared response as a function of angle of incidence. For measurements of sound pressure squared $f(\theta)$ is equal to 1. For measurements of sound power propagating down a duct, $f(\theta)$ is equal to $\cos\theta$, since the sound power is proportional to the projection of the duct

cross-sectional area onto a plane perpendicular to the direction of propagation of the sound. This projected area is proportional to $\cos\theta$.

For equal energy from every angle of incidence, $w(\theta)$ is constant. For equal energy from every element of solid angle, $w(\theta)$ is proportional to $\sin(\theta)$. For every mode with equal energy density, $w(\theta)$ is proportional to the number of modes per unit angle of incidence. If every mode carries equal power down the duct, then the modal energy densities are proportional to $1/\cos\theta$ since the power carried down the duct is proportional to $\cos\theta$. In this case, $w(\theta)$ is proportional to the number of modes per unit angle of incidence divided by the cosine of the angle of incidence.

The correction factor C is the factor by which the desired values are greater than the values measured with the microphone turbulence screen. Thus, the values measured with the microphone turbulence screen must be multiplied by the correction factor. In practice, the correction factor will be expressed in decibels and will be added to the measured sound pressure level. Since the correction factor will usually be positive, applying it will normally mean increasing the measured sound pressure level.

The formula for the number of modes per unit angle of incidence will be derived for a rectangular cross-section duct, since it is well known that the formula for the number of cross-modes depends asymptotically only on the area of the cross-section and the wavenumber. (See for instance Balian and Bloch [9] and note that area is the two-dimensional equivalent of three-dimensional volume.)

If the size of a rigid-walled rectangular duct cross-section is a_y by a_z, the modal wavenumber vectors $\mathbf{k}_{mn}$ of the cross-modes are $(m\pi/a_y, n\pi/a_z)$, where m and n are any non-negative integers. The $\mathbf{k}_{mn}$ form a regular lattice in the first quadrant of the k_y k_z plane with each point occupying an area in this two-dimensional $\mathbf{k}$ space of π^2/S, where $S = a_y a_z$ is the cross-sectional area of the duct. The area of the first quadrant containing wavenumber vectors $\mathbf{k}$ whose magnitude is less than k_p is $\pi {k_p}^2/4$. Thus, the number of modal wavenumber vectors less than k_p is $S{k_p}^2/(4\pi)$. The modal wavenumber vectors $\mathbf{k}_{m0}$ and $\mathbf{k}_{0n}$ which lie on the k_y and k_z axes have only been half-counted since half their area lies in other quadrants. The total number of modal wavenumber vectors on an axis is $(a_y + a_z)k_p/\pi$, and counting an extra half for each of these vectors gives the total number N of modal wavenumber vectors less than k_p, for the square case a_y equals a_z, as

$$N(k_p) = \frac{k_p^2 S + 4k_p\sqrt{S}}{4\pi}. \tag{36}$$

The number of modes per unit of wavenumber magnitude is

$$\frac{\mathrm{d}N}{\mathrm{d}k_p} = \frac{2k_p S + 4\sqrt{S}}{4\pi}. \tag{37}$$

For a mode propagating down the duct, the square of the magnitude of its modal wavenumber is

$$k^2 = k_x^2 + k_p^2, \tag{38}$$

where k_p is the magnitude of the projection of its modal wavenumber vector onto the cross-sectional area of the duct. Now $k_p = \mathrm{k}\sin\theta$ where θ is the angle between the direction of propagation of the mode and the centre line of the duct. Thus $\mathrm{d}k_p/\mathrm{d}\theta = k\cos\theta$. Hence, the number of modes per radian is

$$w(\theta) = \frac{\mathrm{d}N}{\mathrm{d}k_p}\frac{\mathrm{d}k_p}{\mathrm{d}\theta} = \frac{k^2 S\,\sin\,2\theta + 4k\sqrt{S}\,\cos\,\theta}{4\pi}. \tag{39}$$

If every mode carries equal power down the duct, the weighting function is obtained by dividing the number of modes per radian by the cosine of the angle of incidence. This gives

$$w(\theta) = \frac{2k^2 S\,\sin\,\theta + 4k\sqrt{S}}{4\pi}. \tag{40}$$

In actual calculations with Eqs. (39) and (40), k will be approximated with k_0.

Because the modulus squared of Eq. (23) cannot be integrated analytically, the integral in the denominator of Eq. (35) must be integrated numerically. In this report, the trapezoidal rule was used with steps of 5°.

However for the choices of $f(\theta)$ and $w(\theta)$ given above, the integral in the numerator of Eq. (35) can be integrated analytically:

1. For $w(\theta) = 1$ and $f(\theta) = 1$,

$$\int_0^{\pi/2} f(\theta)w(\theta)\,\mathrm{d}\theta = \frac{\pi}{2}. \tag{41}$$

2. For $w(\theta) = 1$ and $f(\theta) = \cos\theta$,

$$\int_0^{\pi/2} f(\theta)w(\theta)\,\mathrm{d}\theta = 1. \tag{42}$$

3. For $w(\theta) = (k^2S \sin 2\theta + 4k\sqrt{S} \cos\theta)/(4\pi)$ and $f(\theta) = 1$,

$$\int_0^{\pi/2} f(\theta)w(\theta)\,\mathrm{d}\theta = \frac{k^2S + 4k\sqrt{S}}{4\pi}. \tag{43}$$

4. For $w(\theta) = (k^2S \sin 2\theta + 4k\sqrt{S} \cos\theta)/(4\pi)$ and $f(\theta) = \cos\theta$,

$$\int_0^{\pi/2} f(\theta)w(\theta)\,\mathrm{d}\theta = \frac{2k^2S + 3\pi k\sqrt{S}}{12\pi}. \tag{44}$$

5. For $w(\theta) = \sin(\theta)$ and $f(\theta) = 1$,

$$\int_0^{\pi/2} f(\theta)w(\theta)\,\mathrm{d}\theta = 1. \tag{45}$$

6. For $w(\theta) = \sin(\theta)$ and $f(\theta) = \cos\theta$,

$$\int_0^{\pi/2} f(\theta)w(\theta)\,\mathrm{d}\theta = \frac{1}{2}. \tag{46}$$

7. For $w(\theta) = (2k^2S \sin\theta + 4k\sqrt{S})/(4\pi)$ and $f(\theta) = 1$,

$$\int_0^{\pi/2} f(\theta)w(\theta)\,\mathrm{d}\theta = \frac{2k^2S + 2\pi k\sqrt{S}}{4\pi}. \tag{47}$$

8. For $w(\theta) = (2k^2S \sin\theta + 4k\sqrt{S})/(4\pi)$ and $f(\theta) = \cos\theta$,

$$\int_0^{\pi/2} f(\theta)w(\theta)\,\mathrm{d}\theta = \frac{k^2S + 4k\sqrt{S}}{4\pi}. \tag{48}$$

If the weighting function is relatively constant, the integrals in Eq. (35) are basically measures of angular bandwidth. This means that directivity values, which are more than 3 dB down will have little effect on the correction factor C. Thus, for determining the correction factor C it does not matter greatly if our predictions or measurements of directivity are in error for those values, which are more than 3 dB down.

The modulus squared of Eq. (23) has to be evaluated for third octave bands of noise. For those frequencies where the rate of change of Eq. (23) as a function of frequency across the third octave band is relatively constant it is sufficient to evaluate the modulus squared of Eq. (23) at the centre frequency of the third octave band. Eq. (23) contains oscillating exponential functions with arguments of the form $\mathrm{i}k_xL$ or $\mathrm{i}k_1L$. For low

Mach numbers, k_x and k_1 are approximately equal to or less than k_0. By the sampling theorem, a new evaluation point should be used at least every time $k_0 L$ increases by π. Thus, the number of points used to calculate a third octave band average is given by

$$N = 1 + \text{int}[(2^{1/6} - 2^{-1/6})k_0 L/\pi], \tag{49}$$

where int() is the function that produces the integer part of a number. The average of the modulus squared of Eq. (23) is averaged over the N values of k_j given by

$$k_j = k_c 2^{(2j-N-1)/(6N)}, \tag{50}$$

where k_c is the value of k_0 at the centre frequency of the third octave band.

Since the microphone turbulence screen integrates in the sound pressure domain, the effective length of the microphone turbulence screen slit can be estimated by integrating $e^{-\beta_1 x}$ over the length of the slit from x equals zero to x equals L. If the effective length is divided by the length L of the slit it gives the effective length ratio

$$F = (1 - e^{-\beta_1 L})/(\beta_1 L). \tag{51}$$

This gives the fraction of the slit length over which the microphone turbulence screen appears to effectively sample.

4. Waterhouse correction

If we only wish to measure the sound pressure squared, or the sound intensity in the direction parallel to the centre line of the duct, at the position of the microphone turbulence screen in the duct, then the modal and velocity corrections derived in the previous section are all that need be applied. However, we usually wish to estimate the sound pressure squared or the sound intensity averaged across the entire cross-sectional area of the duct. In this situation, it is necessary to apply a Waterhouse [10] correction to account for the fact that the sound pressure is greater near the walls of the duct, because of the increase in sound pressure that occurs when sound is reflected at a rigid surface. In a duct, unlike in a reverberation room, the microphone will often be in the interference pattern created near the duct wall by the reflections. This means that the distance of the microphone from the duct wall must also be taken into account.

If we have a plane wave of unit amplitude incident upon a rigid surface in the $x\,z$ plane from the positive y half-space, its sound pressure will be given by the equation

$$p_i = e^{i(\omega t - k_x x + k_y y - k_z z)} \tag{52}$$

and the reflected sound pressure wave will be

$$p_r = e^{i(\omega t - k_x x - k_y y - k_z z)}. \tag{53}$$

At time $t = 0$, the sound pressure on the positive y-axis ($x = 0$, $y > 0$, $z = 0$) will be the sum of p_i and p_r. Thus, the sound pressure is

$$p = e^{ik_y y} + e^{-ik_y y} = 2\cos(k_y y) \tag{54}$$

and the modulus squared of the sound pressure is

$$|p|^2 = 4\cos^2(k_y y) = 2[\cos(2k_y y) + 1]. \tag{55}$$

The average value of the modulus of the sound pressure squared is

$$\langle |p|^2 \rangle = 2 \tag{56}$$

and normalising Eq. (55) by dividing by Eq. (56), gives

$$\frac{|p|^2}{\langle |p|^2 \rangle} = 1 + \cos(2k_y y). \tag{57}$$

Propagating rectangular duct modes with wavenumber k have values of k_y and k_z, which lie uniformly spread in the quarter circular quadrant in the k_y k_z plane bounded by

$$k_y \geqslant 0, \quad k_z \geqslant 0, \quad k_y^2 + k_z^2 \leqslant k^2. \tag{58}$$

The area of this quarter circle quadrant is $\pi k^2/4$. The area of this quadrant with values of k_y between q and $q + \Delta q$ is $\sqrt{k^2 - q^2}\Delta q$. Thus, if all propagating modes have the same amplitude and are uncorrelated, the average value of Eq. (57) over all propagating modes is

$$H = \frac{4}{\pi k^2} \int_0^k \sqrt{k^2 - k_y^2}[1 + \cos(2k_y y)]\, \mathrm{d}k_y. \tag{59}$$

Performing the integration yields

$$H = 1 + \frac{J_1(2ky)}{ky}, \tag{60}$$

where $J_1()$ is the Bessel function of the first kind of order one. The average increase in pressure squared across the duct due to the reflection at one duct wall is

$$\langle H \rangle = \frac{1}{a_y} \int_0^{a_y} \left(1 + \frac{J_1(2ky)}{ky}\right) \mathrm{d}y = 1 + \frac{1}{a_y} \int_0^{a_y} \frac{J_1(2ky)}{ky}\, \mathrm{d}y. \tag{61}$$

For values of k for which ka_y is less than π, cross-modes with a non-zero wavenumber component in the direction of the y-axis cannot exist. In this situation H is equal to one. The integrand of the last integral in Eq. (61) is an oscillating function which decays rapidly as ky increases. For values of k for which ka_y is greater than or equal to π, this integral can be approximated by replacing the upper limit of the integral with plus infinity. This gives

$$\langle H \rangle = 1 + \frac{1}{a_y} \int_0^{\infty} \frac{J_1(2ky)}{ky}\, \mathrm{d}y = 1 + \frac{1}{ka_y}. \tag{62}$$

Taking account of the other three duct walls and ignoring interactions at the four corners gives

$$\langle H \rangle = 1 + \frac{2}{ka_y} + \frac{2}{ka_z}, \tag{63}$$

where the second and/or third terms are set equal to zero if ka_y and/or ka_z are less than π.

The second term of Eq. (60) is an oscillating function, which decays rapidly with increasing distance. If the sound pressure squared is measured at a distance d from the duct wall such that kd is much greater than π, then H is approximately equal to one, and the measured sound pressure squared must be multiplied by Eq. (63) to obtain the average sound pressure squared across the duct. In practice, the microphone will often be closer to the duct walls than π/k and the measured pressure squared has to be corrected for the position of the microphone using Eq. (60). If the microphone is moved over a rectangle whose sides are at a distance of d_y and d_z from the walls of the duct in the direction of the y and z axes, the dimensions of the measurement rectangle are $a_y - 2d_y$ and $a_z - 2d_z$. Using Eq. (60) for each side of the measurement rectangle and the side of the duct nearest to it, and averaging with a weighting equal to the length of the side of the measurement rectangle, gives

$$H = 1 + \frac{(a_z - 2d_z)J_1(2kd_y)}{(a_y + a_z - 2d_y - 2d_z)kd_y} + \frac{(a_y - 2d_y)J_1(2kd_z)}{(a_y + a_z - 2d_y - 2d_z)kd_z}. \tag{64}$$

If the ratio of the width of the measurement rectangle to the width of the duct is the same in both the y and z axes directions, the ratio will be called the relative radius and denoted by R. In this case, Eq. (64) can be written as

$$H = 1 + \frac{2a_z J_1(ka_y[1 - R])}{(a_y + a_z)ka_y(1 - R)} + \frac{2a_y J_1(ka_z[1 - R])}{(a_y + a_z)ka_z(1 - R)}. \tag{65}$$

If ka_y and/or ka_z are less than π, the corresponding $J_1()$ function is set to zero since there are no cross-modes with wavenumber components in that direction. Because the $J_1()$ function oscillates, when calculating third octave band average values, it is set to zero for values of its argument greater than its second positive zero. Its second positive zero is 7.0. Thus, to estimate the average sound pressure squared across the cross-sectional area of the duct, it is necessary to divide the measured sound pressure squared by Eq. (65) and multiply it by Eq. (63).

Values for circular ducts are calculated using a square cross-sectioned duct of the same area. According to Morse and Ingard [11], the cut on frequency of the first cross-mode in a cylindrical duct is 0.5861 c/D where D is the diameter of the duct. The cut on frequency of the first cross-mode for a square cross-sectioned duct with the same cross-sectional area as the cylindrical duct is $c/(\sqrt{\pi}D) = 0.5642c/D$. This differs by less than 4% from the true cylindrical value. Thus, approximating a cylindrical with a square cross-sectioned duct is unlikely to lead to large errors.

5. Experimental directivity

Research work on the directivity of microphone turbulence screens has been dominated by an empirical expression developed at Purdue University. The expression is [1,2,12–14]

$$\frac{p(\theta)}{p(0)} = \frac{1}{1 + kL\theta^3 K} = \frac{1}{1 + f\theta^3 K'}, \tag{66}$$

where the empirical constants K and K' are related by the equation

$$K' = \frac{2\pi LK}{c}. \tag{67}$$

The values of the constant will be given for the case where the angle of incidence θ is expressed in radians. According to Bolleter [12], Flory and Crocker [13] originally developed the second version of Eq. (66) with a value of K' equals 0.00035 for frequencies below 2 kHz. Bolleter then states that it was later found that K' equals 0.00045 gave a better approximation. The first form of Eq. (66) was given by Bolleter et al. [14] with K equals 0.061 below 2 kHz. K equals 0.061 corresponds to Bolleter's value of K' equals 0.00045 for a temperature of 20 °C and a slit length of 400 mm. It should be noted that none of these researchers claimed that the empirical formula could be used above 2 kHz.

The ISO standard 5136 [1,2] gives upper and lower limits for directivity. The upper limit uses Flory and Crocker's value of K' equals 0.00035 for frequencies of 1, 2, 4 and 8 kHz. The lower limit uses K' equals 0.0015 for 1 and 2 kHz, and K' equals 0.0022 for 4 and 8 kHz. Neise et al. [15] used the value of K' equals 0.0005. The values of the empirical constants K and K' for a temperature of 20 °C and a slit length of 400 mm are shown in Table 1.

A serious problem with the empirical formula (66) that will become apparent later in this paper is that it does not include the flow velocity of the air in the duct. This leads to the contradiction that while the modal corrections in ISO 5136:1990 [1] are calculated for a duct with no flow using Eq. (66), the velocity corrections are calculated for a duct with no cross-modes using Neise's version of Eq. (26). It will be shown later that this approach leads to large errors in the total correction factor at the high frequencies. It is also more satisfactory to use theoretical directivity formulae like Eqs. (23)–(26) rather than an empirical formula like Eq. (66).

Table 1
Values of the empirical directivity constants K and K' for a temperature of 20 °C and a slit length of 400 mm

Source	K	K'
Flory and Crocker <2 kHz, ISO upper limit	0.048	0.00035
Bolleter <2 kHz, Bolleter, Cohen and Wang <2 kHz	0.061	0.00045
Neise, Frommhold, Mechel and Holste	0.068	0.00050
ISO lower limit <4 kHz	0.205	0.0015
ISO lower limit ⩾4 kHz	0.300	0.0022

Indeed, the main aim of this section is to show that the theoretical Eqs. (23)–(26) are in better agreement with the experimental results than Eq. (66).

The directivities of three microphone turbulence screens were measured in an anechoic room using third octave bands of random noise from 50 Hz to 10 kHz. The lining and testing of this anechoic room has already been described in the journal literature [16,17]. A 300 mm diameter dual cone loudspeaker mounted in a baffle was placed 3.6 m from the centre of the microphone turbulence screen slit with the axis of the loudspeaker on the line joining the loudspeaker and the microphone turbulence screen. The loudspeaker was driven with pink noise, which was passed through a third octave graphic equaliser set to boost the high- and low-frequency noise. The measured results were corrected for the effects of background noise. The frequency response of the microphone turbulence screens was measured from 0° to 75° in steps of 15°. The directivity relative to the 0° response was then calculated for 15° to 75° in steps of 15°. The values of the directivity expressed in decibels calculated using the different formulae were subtracted from the experimental directivity in decibels. The root mean square (rms) value of the 120 differences in decibels (24 frequencies times 5 angles) was calculated for each of the formulae. The results for three different microphone turbulence screens and the rms values across all three microphone turbulence screens (360 differences) are shown in Table 2.

The results for a Brüel and Kjær Type UA0436 microphone turbulence screen are shown in column 2 of Table 2. The theoretical directivity value used in the last row was calculated using Eqs. (24) and (34). A value of 369 mks rayls was measured in situ for the specific airflow resistance of the material covering the slit. This value of specific airflow resistance was used in the theoretical calculations. The empirical equation (66) and the different empirical constants shown in Table 1 were used for the other rows.

Directivity measurements were also made on a microphone turbulence screen with anechoic terminations at both ends of the slit [7,8]. The anechoic terminations consisted of 30 m of plastic tubing with the same internal cross-sectional area as the slit tube. The microphone was flush mounted in the wall of the tube so that it caused no reflections. The slit was 500 mm long and 1 mm wide. The internal cross-section of the slit tube was rectangular and measured 11.2 mm × 11.8 mm. Measurements were made with two different values of specific airflow resistance material covering the slit. Column 3 of Table 2 shows the results for a specific airflow resistance extrapolated to zero flow rate of 332 mks rayls. Column 4 shows the results for 493 mks rayls. The theoretical results were calculated using Eq. (23) with a value of a equals 1 and Eq. (34). The empirical values were calculated using the first part of Eq. (66) with a slit length L of 500 mm. The values of K were calculated from the K' values using Eq. (67) with a temperature of 20 °C and L equals 400 mm.

Examination of Table 2 shows that the theoretical directivity equation agrees much better with the experimental directivity results than any of the versions of the empirical directivity equation. This implies that the theoretical directivity equation should be used instead of the empirical directivity equation when calculating the modal correction factor.

When the individual directivity values were examined, none of the microphone turbulence screens completely satisfied the ISO upper and lower limiting directivity equations. Thus, there is a need to revise these equations in ISO 5136 [1,2].

Table 2
The rms values of the differences in decibels between the experimental third octave noise directivity and the calculated directivity using different formulae

	Brüel & Kjær Type UA 0436	Anechoic 332 mks rayl	Anechoic 493 mks rayl	Over all 3 screens
ISO upper	5.9	3.3	4.3	4.6
Bolleter et al.	5.3	2.8	3.8	4.1
Neise et al.	5.0	2.6	3.6	3.8
ISO lower	2.4	4.2	3.9	3.6
Theory	2.2	1.3	2.0	1.9

The range is the third octave band frequencies from 50 Hz to 10 kHz inclusive and the angles of incidence from 15° to 75° in 15° steps. Results are given for three different microphone turbulence screens and over all 3 microphone turbulence screens.

6. Modal correction factors with no flow

Previously modal correction factors for ducts with no flow have been calculated using what will be referred to as the deterministic method. The modal sound pressure squared due to each propagating mode has been calculated at a point on the measurement path. The empirical directivity formula of the microphone turbulence screen has then been applied to each modal pressure squared using the angle of incidence of the mode and the results added together to give the total sound pressure squared at the point, using the assumption that the modes are uncorrelated. The total sound pressure squared was then averaged over a number of points on the measurement path. This averaged total sound pressure squared was used to calculate the sound power being propagated down the duct by assuming that only plane wave propagation was occurring.

The sound power carried down the duct by each mode was also calculated and the results added together to give the actual sound power propagating down the duct. The correction factor was given by the difference between the actual sound power and the sound power calculated from the averaged total sound pressure squared using the plane wave propagation assumption. The calculated correction factors were then averaged over a number of frequencies in each third octave band. This deterministic method does involve averaging over the circular traverse and the third octave band of frequencies. Since it is applied to a range of duct diameters, it should also involve averaging over duct diameters. It is very demanding computationally and it takes longer to complete the calculations at high frequencies in large cross-sectional area ducts because the number of propagating modes becomes large. According to Holste and Neise [18], the calculated modal correction factors were extrapolated to higher frequencies and larger duct diameters for use in ISO 5136:1990 [1].

The method of calculating the modal correction factor described in Section 3 will be referred to in this paper as the statistical method. Its advantage is that it does not need very much computing. The results from the statistical method presented in this paper were performed in a spreadsheet.

According to Neise et al. [15], the modal correction factors in ISO 5136:1990 [1] were calculated using the assumption that each mode carries equal sound power down the duct. This assumption is equivalent to the assumption that the average over the cross-sectional area of each modal sound pressure squared is proportional to $1/\cos\theta$, where θ is the angle of the direction of propagation of the mode to the centre line of the duct. If each mode has equal energy density, the average mentioned in the last sentence is constant across modes.

In ISO 5136:1990 [1], modal corrections are given for six different ranges of circular cross-section duct diameters. The smallest three ranges in the standard use a relative measurement radius of R equals 0.8, whilst

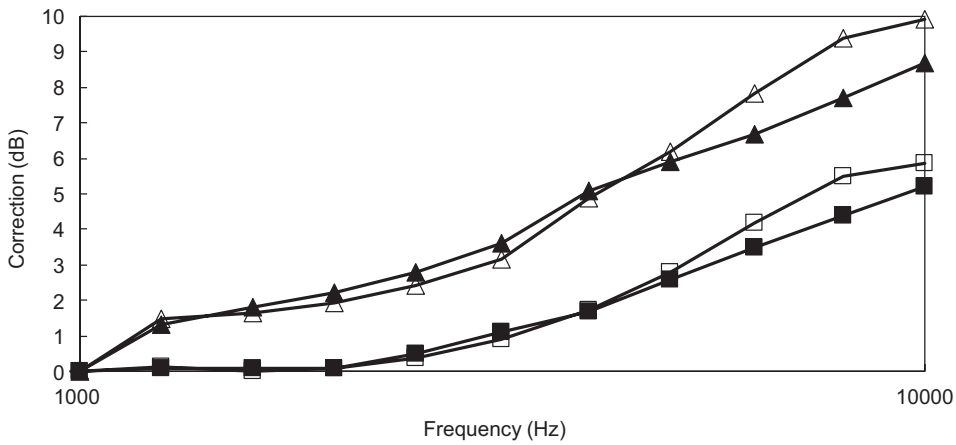

Fig. 2. Comparison of the modal corrections for no flow calculated by Bolleter with those for a duct diameter of 0.16 m. Bolleter and lower directivity limit ▲, statistical method and lower directivity limit △, Bolleter and upper directivity limit ■, statistical method and upper directivity limit □.

the largest three ranges use a relative measurement radius of R equals 0.65. Bolleter calculated the modal correction factors using the deterministic approach for both the upper and lower directivity limit curves given in ISO 5136:1990 [1]. The modal corrections in ISO 5136:1990 [1] lie on a smooth curve roughly half way between the modal correction curves for the upper and lower directivity limits. The ISO 5136:1990 [1] corrections were limited to a minimum value of 0 dB and a maximum value of 6 dB. In Fig. 2, Bolleter's calculated modal corrections are compared with modal corrections calculated using the statistical method, the empirical upper and lower directivity limits of ISO 5136:1990 and the assumption that each propagates equal sound power along the duct. At high frequencies, Bolleter's modal corrections are less than those of the statistical method because he limited the inverse cosine increase caused by the assumption of equal modal power to a maximum factor of 3.1. At other frequencies the agreement is reasonably good.

Neise et al. [15] have calculated modal correction factors for rectangular cross-section ducts with aspect ratios of 1:1, 2:1 and 3:1. The larger of the duct cross-section dimensions took the values 0.25, 0.5, 1 and 2 m. Calculations were made for measurement rectangles with relative radii of both 0.4 and 0.6. The empirical directivity equation (66) was used with an empirical constant of K' equals 0.0005. The equal modal energy density model was assumed for the sound energy angular distribution. The calculations were made using the deterministic method described above. For comparison purposes the modal corrections were recalculated with

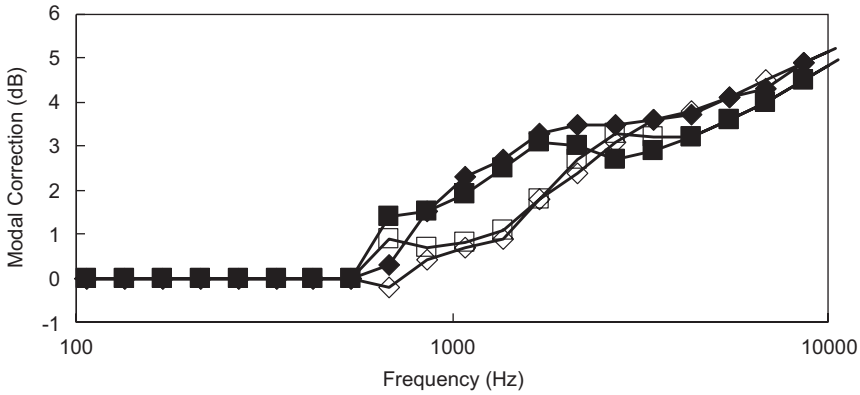

Fig. 3. Comparison of the modal corrections for no flow for a rectangular cross-section duct measuring 0.25 m × 0.25 m. Deterministic method for a relative radius of 0.4 ◆, statistical method for a relative radius of 0.4 ■, deterministic method for a relative radius of 0.6 ◇, statistical method for a relative radius of 0.6 □.

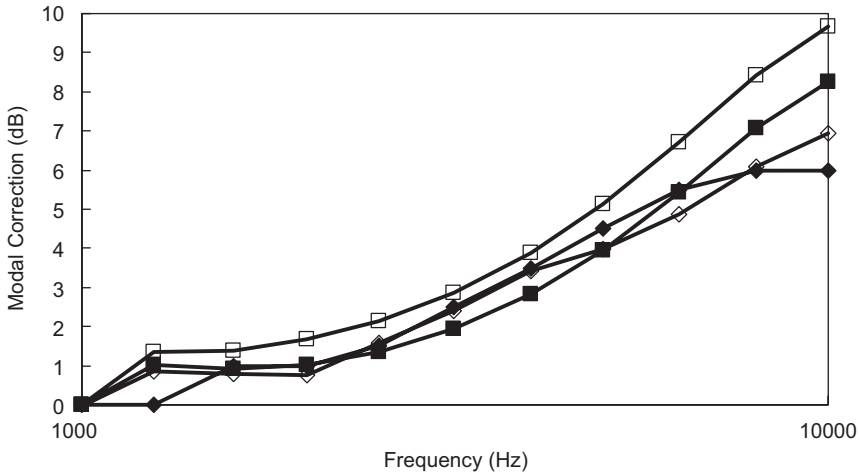

Fig. 4. Comparison of the modal corrections with no flow calculated using the statistical method, theoretical directivity and equal modal power □ or equal modal energy density ■ with ISO 5136:2003 ◇ and ISO 5136:1990 ◆ for a circular duct of diameter 0.16 m.

the statistical method outlined in this paper using the same assumptions for angular sound energy distribution and microphone turbulence screen directivity. A typical result is shown in Fig. 3 for a duct measuring 0.25 m × 0.25 m. It is seen that there is fairly good agreement between the results calculated by the two different methods. However, the deterministic results appear to be systematically larger than the statistical results for the high frequencies. This systematic difference was much smaller for the larger duct sizes. It is believed to be due to the fact that the cross-modes first start propagating at 90° to the axis of the duct as frequency is increased. This means that the discrete individual modes propagate slightly closer to 90° than predicted by the continuous distribution of the statistical approach. Thus the deterministic model produces slightly greater values of modal correction factor than the statistical model because of the directivity of the microphone turbulence screen. As the number of cross-modes increases with increasing frequency and increasing duct size this difference decreases.

It should be pointed out that the results in Fig. 3 are given only for the purpose of comparing the deterministic method with the statistical method. It is believed that the assumptions used give modal correction factors which are too small. In particular, it has already been shown that the empirical directivity equation does not agree as well with the experimental directivity results as the theoretical directivity equation.

Fig. 4 shows the comparison of the modal corrections with no flow calculated using the statistical method, theoretical directivity and equal modal power or equal modal energy density with ISO 5136:2003 and ISO 5136:1990 for a circular duct of diameter 0.16 m. Fig. 4 can be directly compared with Fig. 2. Fig. 4 shows that the assumption of equal modal power gives higher corrections than the assumption of equal modal energy density.

7. Modal correction factors with flow

The combined modal and flow velocity correction for ISO 5136:2003 [2] was calculated by Arnold (see Neise and Arnold [18]). Arnold used the deterministic method with the theoretical rather than the empirical directivity model. He used the assumption of equal modal energy density rather than equal modal power. ISO 5136:2003 [2] gives a combined modal and velocity correction for nose cones and foam balls of

$$-20\ \log(1-M)\,\mathrm{dB}, \tag{68}$$

where M is the Mach number. This correction takes account of the effects of the flow on the propagation of sound power in the duct. It is added to all the theoretical calculations given in this section.

In this section calculated modal correction factors with flow will be compared with experimental measurements on fans made by Holste and Neise and by Bolton. The statistical method will be used with the theoretical directivity given by Eqs. (24) and (34) and the assumption of equal modal energy density (for Holste and Neise and for Bolton) or equal modal power (for Bolton only). The in-situ experimentally measured specific airflow resistance of the material covering the slit of 369 mks rayls was used in these calculations.

The experimental difference between the fan sound power determined in a free field anechoic room and the fan sound power determined in a duct are shown in Figs. 23 and 24 of Ref. [19]. The numerical values for the case without cone were kindly faxed to me by Neise. In this case the values corrected for background noise were used. The values for the case with a cone attached to the fan for the anechoic room measurements were read from Fig. 23 of Ref. [19]. Because the in-duct measurements used in calculating the results would have already had the modal corrections and the flow velocity corrections given by ISO 5136:1990 [1] added to them, these differences are equal to the differences between the experimentally determined correction factors and the ISO 5136:1990 [1] correction factors. In other words, the ISO 5136:1990 [1] correction factors correspond to zero on these graphs. For this reason the modal corrections and flow velocity corrections of ISO 5136:1990 [1] were subtracted from the statistical modal corrections with flow before comparing them with the experimental differences.

The in-duct measurements were made in a duct with an inner diameter of 500 mm. The cut on frequency for the first cross-mode is 400 Hz. Since, in this paper we are not interested in the radiation efficiency of the duct end, the results are presented only from 400 Hz upwards. The results are shown in Figs. 5(a)–(e). Figs. 5(a)–(d) correspond to Figs. 23(a)–(d) of Ref. [19], respectively.

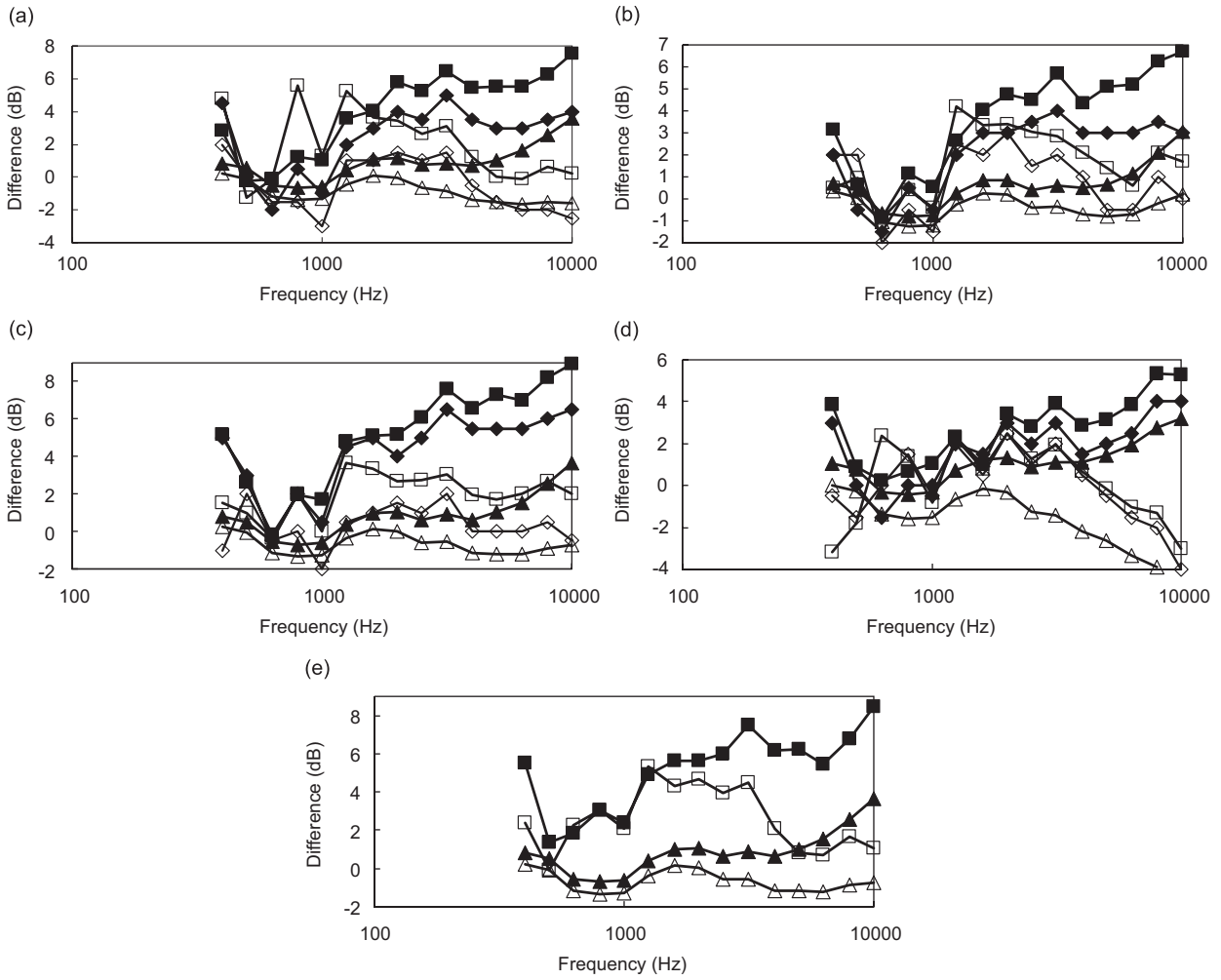

Fig. 5. Comparison of the difference between the experimental or theoretical modal corrections with flow and the combined modal and flow velocity correction of ISO 5136:1990 [1]. Fan (a) is a centrifugal fan with backward curved airfoil blades running at 1900 rev/min and producing a linear velocity of 10.7 m/s in the 500 mm diameter duct. Fan (b) is a centrifugal fan with flat radial blades running at 1800 rev/min and producing a linear velocity of 6.1 m/s in the 500 mm diameter duct. Fan (c) is a centrifugal fan with forward curved blades (scirrocco blower) running at 700 rev/min and producing a linear velocity of 9.2 m/s in the 500 mm diameter duct. Fan (d) is an axial flow fan with airfoil blades and outlet guide vanes running at 2970 rev/min and producing a linear velocity of 16.8 m/s in the 500 mm diameter duct. Fan (e) is a centrifugal fan with backward curved sheet metal blades running at 1600 rev/min and producing a linear velocity of 9.2 m/s in the 500 mm diameter duct. Except for fan (e), the experimental results are given for the fans with and without a cone attached when the anechoic room measurements were made. Experimental outlet duct without cone ■, experimental outlet duct with cone ◆, theoretical outlet duct ▲, experimental inlet duct without cone □, experimental inlet duct with cone ◇, theoretical inlet duct △.

Both inlet and outlet measurements are shown. The theoretical results and the experimental results with and without cone show that there is a big difference between the corrections for outlet ducts and inlet ducts, since the ISO 5136:1990 [1] corrections, which correspond to zero in graphs, are almost the same for outlet and inlet ducts. In ISO 5136:1990 [1], most of the small differences that occur are in the wrong direction with the inlet corrections being larger than the outlet corrections. The reason for this error is that Eqs. (24) and (34) show that it is not possible to separate the modal corrections and the velocity corrections as has been done in ISO 5136:1990 [1]. The effect of the flow in the outlet duct is to decrease the wavenumber component parallel to the axis of the duct (see Eq. (34)). This makes the turbulence screen more directional and the correction factor larger for a given measurement frequency. In the inlet duct, the flow increases the component of the

wavenumber which is parallel to the axis of the inlet duct. This makes the turbulence screen less directional and the correction factor smaller for a given measurement frequency.

Apart from the axial flow fan in Fig. 5(d) (which also produced the highest linear flow velocity in the measurement duct), the experimental results are generally significantly greater than the theoretical results. Nevertheless, the theoretical results are in the right direction and substantially reduce the discrepancy especially for outlet ducts at high frequencies. The theoretical and experimental inlet duct values are closer to the ISO 5136:1990 [1] values (zero on these figures) than the outlet duct values.

Bolton [20] made measurements in a 610 mm diameter inlet duct with a Brüel and Kjær microphone turbulence screen type UA 0436 and a Brüel and Kjær 12.7 mm microphone nose cone type UA 0386 at a relative radius of R equals 0.65, and with a Brüel and Kjær polyurethane foam ball windscreen type UA 0237 and a Brüel and Kjær 12.7 mm microphone nose cone type UA 0386 at a relative radius of R equals 0.5. The linear flow velocity in the duct was 13.7 m/s. The difference in relative radius was ignored since all three non-microphone turbulence screen measurements were similar. The three non-microphone turbulence screen

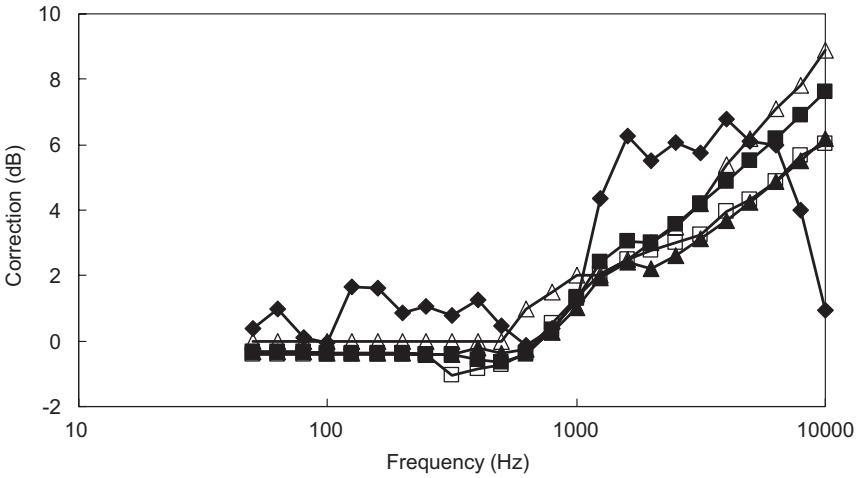

Fig. 6. The difference between the average of measurements made with a nose cone at relative radii of 0.5 and 0.65 and a foam ball windscreen at a relative radius of 0.5, and the measurements made with a microphone turbulence screen at a relative radius of 0.65. The measurements were made in the 610 mm diameter inlet duct of a fan. The difference ◆ is compared with the statistical modal correction with flow for equal modal power ■ and equal modal energy density ▲, and the combined modal and flow velocity correction from ISO 5136:2003 □ and ISO 5136:1990 △.

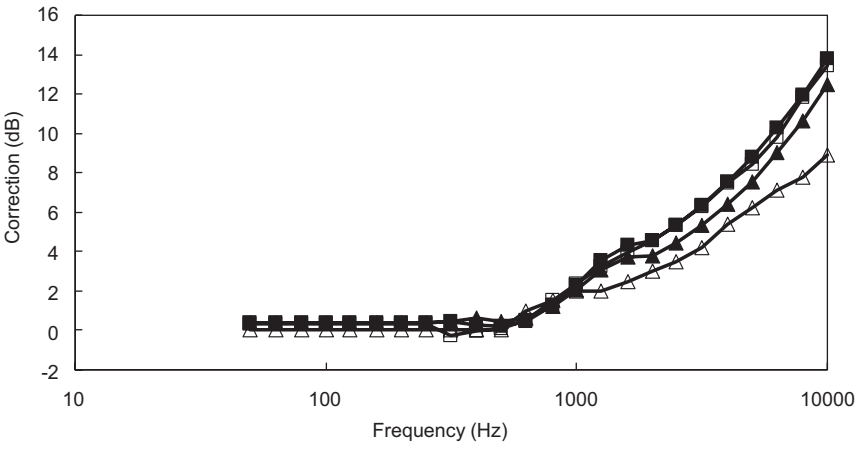

Fig. 7. Comparison of the combined modal and flow velocity corrections for a 610 mm diameter outlet duct with a flow velocity of 13.7 m/s. Statistical method with equal power ■, statistical method with equal modal energy density ▲, ISO 5136:2003 □ and ISO 5136:1990 △.

Table 3
Differences between modal and velocity corrections from ISO 5136:2003 and those calculated using the statistical method of this paper

Velocity (m/s)	−30	−15	−5	5	15	30
Average (dB)	−0.3	−0.1	0.1	0.2	0.3	0.3
Standard deviation (dB)	0.4	0.4	0.4	0.5	0.5	0.6
Maximum (dB)	0.6	0.8	0.8	0.8	1.0	1.3
Minimum (dB)	−1.0	−1.0	−1.0	−1.0	−1.0	−1.0

measurements were averaged and the microphone turbulence screen measurements were subtracted from this average to give an experimental estimate of the modal correction factor with flow. The theoretical results are calculated with the statistical method using the theoretical directivity formulae (24) and (34) and the assumption of equal sound power propagation down the duct by each mode or equal modal energy density. The cut on frequency for the first cross-mode is 330 Hz.

The experimental and theoretical corrections are shown in Fig. 6 together with the combined corrections from ISO 5136:1990 [1] and ISO 5136:2003 [2]. In this inlet duct the theory and both standards produce fairly similar corrections. (This would not be the case in the outlet duct at this flow rate as is shown in Fig. 7.) The trend of these corrections is the same as the experimental results, but they significantly underestimate the experimental results in the 1.25–4 kHz range and overestimate the experimental results above 5 kHz. This underestimation and overestimation is believed to be due to the actual angular distribution of the incident sound power on the microphone turbulence screen being different from that assumed in the theoretical models.

The modal and flow velocity corrections given in Table D.1 of ISO 5136:2003 [2] were compared with those calculated using the statistical method developed in this paper. The assumptions were the same as those used by Arnold. In particular, the specific airflow resistance of the material covering the slit was assumed to be equal to the characteristic impedance of air and the modes were assumed to have equal energy density. The mean, standard deviation, maximum and minimum values of the differences across the third octave band frequencies from 50 Hz to 20 kHz were calculated for each of the six different flow rates. The results are given in Table 3. The reasonable agreement supports the modal and flow velocity corrections given in ISO 5136:2003 [2].

8. Conclusion

This paper has shown that the modal and flow velocity corrections for a microphone turbulence screen should not be separated as is done in the international standard ISO 5136:1990 [1]. The separation of these two corrections leads to large errors in the corrections for outlet ducts. This error has been corrected in ISO 5136:2003 [2].

The empirical directivity equation which is widely used for microphone turbulence screens does not agree well with experimental directivity measurements. It should be replaced with the theoretical directivity equation.

This paper presents a new statistical method of calculating the combined modal and flow velocity corrections for a microphone turbulence screen using a statistical room acoustics style of approach. This new method agrees fairly well with the old deterministic approach for the no flow situation when the same assumptions are used. The advantages of the new method are that it requires much less computing. Although this new method produces modal correction factors with flow which are closer to the experimental results than the corrections in ISO 5136:1990, the experimental results are still significantly different. This is believed to be due to the actual angular distribution of the incident sound power being different from that assumed in the theoretical models. However, the new method does agree reasonably well with the modal and velocity correction factors given in ISO 5136:2003 [2].

Acknowledgements

The author wishes to acknowledge the assistance provided to him by Dr. W. Neise in the form of personal communications, preprints and reprints. He also wishes to acknowledge the contribution of Mr. P. Jenvey who was responsible for the development project out of which grew the work described in this paper.

References

[1] International Organisation for Standardisation ISO 5136, *Acoustics — Determination of Sound Power Radiated into a Duct by Fans — In-Duct Method*, first ed., 1990.

[2] International Organisation for Standardisation ISO 5136, *Acoustics — Determination of Sound Power Radiated into a Duct by Fans and Other Air Moving Devices — In-Duct Method*, second ed., 2003.

[3] W. Neise, Theoretical and experimental investigations of microphone probes for sound measurements in turbulent flow, *Journal of Sound and Vibration* 39 (1975) 371–400.

[4] J.S. Wang, M.J. Crocker, Tubular windscreen design for microphones for in-duct fan sound power measurements, *Journal of the Acoustical Society of America* 55 (1974) 568–575.

[5] A. Michalke, Sensitivity of a slit-tube probe to higher order acoustic modes in a pipe of circular cross-section, *Journal of Sound and Vibration* 151 (1991) 157–162
ERRATA, *Journal of Sound and Vibration* 155 (1992) 571 (Note that l_1 and I_1 in the errata should both be L).

[6] A. Michalke, On the sensitivity of a slit-tube microphone to the higher-order modes and its consequences, *Proceedings of the DGLR/AIAA Aeroacoustics Conference*, Aachen, Germany, Paper DGLR-AIAA-92-02-026, 11–14 May 1992.

[7] J.L. Davy, I.P. Dunn, A flush mounted microphone turbulence screen, Practical Acoustic Solutions—Proceedings of the Australian Acoustical Society 1992 Annual Conference, Ballarat, Victoria, Australia, 25–27 November 1992, pp. 189–202.

[8] J.L. Davy, I.P. Dunn, The development of a flush mounted microphone turbulence screen for use in a power station chimney flue, *Noise Control Engineering Journal* 41 (1993) 313–322.

[9] R. Balian, C. Bloch, Distribution of eigenfrequencies for the wave equation in a finite domain 1. Three-dimensional problem with smooth boundary surface, *Annals of Physics* 60 (1970) 401–447.

[10] R.V. Waterhouse, Interference patterns in reverberant sound fields, *Journal of the Acoustical Society of America* 27 (1955) 247–258.

[11] P.M. Morse, K.U. Ingard, *Theoretical Acoustics*, McGraw-Hill Book Company, New York, 1968.

[12] U. Bolleter, Theory and Measurement of Modal Spectra in Hard-walled Cylindrical Ducts, PhD Thesis, Purdue University, 1970.

[13] L. Flory, M.J. Crocker, Evaluation of two sampling tubes, Herrick Laboratories Report HL70-26, 1970.

[14] U. Bolleter, R. Cohen, J. Wang, Design considerations for an in-duct sound power measuring system, *Journal of Sound and Vibration* 28 (1973) 669–685.

[15] W. Neise, W. Frommhold, F.P. Mechel, F. Holste, Sound power determination in rectangular flow ducts, *Journal of Sound and Vibration* 174 (1994) 201–237.

[16] W.A. Davern, J.A. Hutchinson, Polyurethane ether foam wedges for anechoic chamber, *Applied Acoustics* 4 (1971) 287–302.

[17] J.L. Davy, Evaluating the lining of an anechoic room, *Journal of Sound and Vibration* 132 (1989) 411–422.

[18] W. Neise, F. Arnold, On sound power determination in flow ducts, *Journal of Sound and Vibration* 244 (2001) 481–503.

[19] F. Holste, W. Neise, Experimental comparison of standardised sound power measurement procedures for fans, *Journal of Sound and Vibration* 152 (1992) 1–26.

[20] A.N. Bolton, Further tests to assess the performance of a sampling tube microphone windscreen, National Engineering Laboratory Glasgow Report B/544, 1979.